JPET Fast Forward. Published on September 11, 2012 as DOI: 10.1124/jpet.112.198945

JPET #198945

Title Page

Antagonists of GPR35 display high species ortholog selectivity and varying modes of action

Laura Jenkins, Nicholas Harries, Jennifer E. Lappin, Amanda E. MacKenzie, Zaynab Neetoo-Isseljee, Craig Southern, Edward G. McIver, Stuart A. Nicklin, Debra L. Taylor and Graeme Milligan

Molecular Pharmacology Group, Institute of Molecular, Cell and Systems Biology, (LJ, NH, JEL, AEM, GM) and Institute of Cardiovascular and Medical Sciences (JEL, SAN), College of Medical, Veterinary and Life Sciences, University of Glasgow, Glasgow G12 8QQ, UK and MRC Technology, Centre for Therapeutics Discovery, 1-3 Burtonhole Lane, Mill Hill, London NW7 1AD, UK (ZN-I, CS, EM, DLT)

JPET Fast Forward. Published on September 11, 2012 as DOI: 10.1124/jpet.112.198945
This article has not been copyedited and formatted. The final version may differ from this version.

JPET #198945

Running Title Page

Running title: Species selectivity of GPR35 antagonists

Address correspondence to:

Graeme Milligan, Wolfson Link Building 253, University of Glasgow,

Glasgow G12 8QQ, Scotland, U.K.

Tel +44 141 330 5557

FAX +44 141 330 5841

e-mail Graeme.Milligan@glasgow.ac.uk

manuscript information

Text pages 40

Number of Tables 2

Number of Figures 13

Number of References 34

Words in: Abstract 234, Introduction 581, Discussion 1659

Non-standard abbreviations

BRET, bioluminescence resonance energy transfer; DMEM, Dulbecco's modification of Eagle's medium; GPCR**,** G protein-coupled receptor; PEI, polyethylenimine;

Recommended section

Cellular and Molecular

JPET Fast Forward. Published on September 11, 2012 as DOI: 10.1124/jpet.112.198945
This article has not been copyedited and formatted. The final version may differ from this version.

ABSTRACT

Variation in pharmacology and function of ligands at species orthologs can be a confounding feature in understanding the biology and role of poorly characterized receptors. Substantial selectivity in potency of a number of GPR35 agonists has previously been demonstrated between human and rat orthologs of this G protein-coupled receptor. Via a bioluminescence resonance energy transfer-based assay of induced interactions between GPR35 and β-arrestin-2, addition of the mouse ortholog to such studies indicated that, as for the rat ortholog, murine GPR35 displayed very low potency for pamoate whilst potency for the reference GPR35 agonist zaprinast was intermediate between the rat and human orthologs. This pattern was replicated in receptor internalization and G protein activation assays. The effectiveness and mode of action of two recently reported GPR35 antagonists methyl-5-[(tert-butylcarbamothioylhydrazinylidene)methyl]-1-(2,4-difluorophenyl)pyrazole-4-carboxylate (CID-2745687) and 2-hydroxy-4-[4-(5*Z*)-5-[(*E*)-2-methyl-3-phenylprop-2-enylidene]-4-oxo-2-sulfanylidene-1,3-thiazolidin-3-yl]butanoylamino]benzoic acid (ML-145, CID-2286812) was investigated. Both CID-2745687 and ML-145 competitively inhibited effects of cromolyn disodium and zaprinast at human GPR35, two agonists that share an overlapping binding site. By contrast, although ML-145 also competitively antagonized effects of pamoate, CID-2745687 acted in a non-competitive fashion. Neither ML-145 nor CID-2745687 was able to effectively antagonize agonist effects of either zaprinast or cromolyn disodium at either rodent ortholog of GPR35. These studies demonstrate that marked species selectivity of ligands at GPR35 is not restricted to agonists and that considerable care

is required to select appropriate ligands to explore the function of GPR35 in non-human cells and tissues.

JPET Fast Forward. Published on September 11, 2012 as DOI: 10.1124/jpet.112.198945
This article has not been copyedited and formatted. The final version may differ from this version.

Introduction

GPR35 is a poorly characterized member of the rhodopsin-like, class A subfamily of G protein-coupled receptors (GPCRs) which, based in part on expression pattern, has attracted attention as a possible therapeutic target in conditions ranging from diabetes and cardiovascular disease to inflammation and pain (Milligan, 2011; MacKenzie et al., 2011). There are, however, major challenges in efforts to understand the role of this receptor. These include that kynurenic acid, the first endogenously produced molecule identified as being able to activate GPR35 (Wang et al., 2006), is substantially more potent at the rat ortholog than the human form (Jenkins et al., 2010). This has resulted in suggestions that kynurenic acid may not be a true endogenous regulator of at least the human ortholog, leaving GPR35 still as an 'orphan' receptor (MacKenzie et al., 2011). Although a number of synthetic GPR35 agonists have been identified via various screens (Jenkins et al., 2010; Zhao et al., 2010) in cases where it has been examined, a number of these also display marked variation in potency to activate the human and rat orthologs (Jenkins et al., 2010; Milligan, 2011). Both in drug discovery programmes and in the use of animal models to explore receptor function marked variation in ligand activity and /or in ligand structure-activity relationships pose important challenges, particularly for poorly characterized receptors in which the orthosteric binding site remains undefined. Moreover, although the available literature on ligand activation of this receptor is relatively limited, it is also not entirely consistent. For example, the most potent agonist reported to date at human GPR35 is pamoate (**Figure 1**) (Zhao et al., 2010; Jenkins et al., 2010). However, although pamoate has been reported to also be an

effective agonist at mouse GPR35 (Zhao et al., 2010) it has been reported to show very low activity at the rat ortholog (Jenkins et al., 2010). A further limitation in efforts to understand the function of GPR35 is that until recently no antagonist ligands had been described. Two recent publications have, however, demonstrated that both CID-2745687 (**Figure 1**) (Zhao et al., 2010) and ML-145 (**Figure 1**) (Heynen-Genel et al., 2010) are antagonists.

Because of the potential differences in responses of rat and mouse GPR35 to pamoate (Jenkins et al., 2010; Zhao et al., 2010) and the high potency of this ligand at the human ortholog we have re-assessed ligand selectivity at these three orthologs and considered the potential usefulness of the reported GPR35 antagonists to unravel the physiological roles of this receptor. Using each of a bioluminescence resonance energy transfer (BRET)-based GPR35-β-arrestin-2 interaction assay, a receptor internalization assay and generation of intracellular inositol phosphates via co-expression of chimeric G proteins we demonstrate that pamoate is highly selective for human GPR35 compared to either of the rodent orthologs. Furthermore, although CID-2745687 (Zhao et al., 2010) and ML-145 (Heynen-Genel et al., 2010) act as effective antagonists at human GPR35 neither displays significant activity at either rodent ortholog. Finally, although ML-145 acts as a competitive antagonist for a number of agonists at human GPR35, CID-2745687, whilst a competitive antagonist of the agonist actions of both zaprinast and cromolyn disodium, antagonizes the agonist effect of pamoate at human GPR35 in a non-competitive manner.

These studies highlight a number of the challenges in exploring both the basis of ligand binding and in potentially understanding the function of poorly characterized

JPET Fast Forward. Published on September 11, 2012 as DOI: 10.1124/jpet.112.198945
This article has not been copyedited and formatted. The final version may differ from this version.

receptors such as GPR35 and demonstrate that considerable care is required to select appropriate ligands to explore the function of GPR35 in non-human cells and tissues.

MATERIALS AND METHODS

Materials – Materials for cell culture were from Sigma-Aldrich (Gillingham, Dorset, UK) Invitrogen (Paisley, Strathclyde, UK), or PAA Laboratories Ltd (Yeovil, Somerset, UK). Polyethylenimine (PEI), linear MW-25000 was from Polysciences Inc (Warrington, PA, USA). Zaprinast, methyl-5-[(tert-butylcarbamothioylhydrazinylidene)methyl]-1-(2,4-difluorophenyl)pyrazole-4-carboxylate (CID-2745687) and 2-hydroxy-4-[4-(5*Z*)-5-[(*E*)-2-methyl-3-phenylprop-2-enylidene]-4-oxo-2-sulfanylidene-1,3-thiazolidin-3-yl]butanoylamino]benzoic acid (ML-145) were from Tocris Bioscience (Bristol, UK). Cromolyn disodium, pamoate and Hoechst 33258 solution were from Sigma-Aldrich (Gillingham, Dorset). Ligands were initially dissolved in DMSO and then diluted in assay buffer.

***GPR35* constructs -** A FLAG epitope (DYKDDDDK) was introduced in the N-terminal end of each of human, rat and mouse GPR35 cDNA by PCR using the following primers: human sense, 5’GCGAAGCTTGCCACCATGGATTACAAGGATGACGACGATAAGAATGGC ACCTACAACACC 3’, rat sense, 5’CGCGGATCCGCCACCATGGATTACAAGGATGACGACGATAAGAACAAT ACAAATTGTAGCATC 3’; mouse sense, 5’TTTTGGATCCGCCACCATGGATTACAAGGATGACGACGATAAGATGAAT AGTACAACCTGTAACAGCACC 3’ and human antisense,

JPET Fast Forward. Published on September 11, 2012 as DOI: 10.1124/jpet.112.198945
This article has not been copyedited and formatted. The final version may differ from this version.

5'GGCCGCGGCCGCCTCTAGAATTAGGCGAGGG 3', rat antisense, 5'GGCCGCGGCCGCCGGTGAGGCTCAGGCTCTG 3' and mouse antisense, 5'TTTTGCGGCCGCGGTGAGGCTCAGGATCTGG 3'.

The HindIII, BamHI and NotI restriction sites used for cloning are underlined. The resulting cDNA was subsequently cloned in frame into the HindIII/BamHI and NotI sites of an eYFP-pcDNA5/FRT/TO plasmid yielding the final N-terminal epitope and C-terminal fluorescence tagged constructs -human FLAG-GPR35-eYFP-pcDNA5/FRT/TO, rat FLAG-GPR35-eYFP-pcDNA5/FRT/TO and mouse FLAG-GPR35-eYFP-pcDNA5/FRT/TO. The integrity of each fusion was checked by DNA sequencing.

G protein chimeras

The chimeric $G_{q-i}(5)$ or $G_{q-13}(5)$ Gα subunits in which the C-terminal 5 amino acids of $G\alpha_q$ were replaced by the corresponding amino acids from either $G\alpha_{i1/2}$ or $G\alpha_{13}$ were described in Jenkins et al., (2011).

Cell culture and transfection - Flp-In™ TREx™ 293 cells (Invitrogen) were maintained in Dulbecco's modification of Eagle's medium (DMEM) without sodium pyruvate (Invitrogen), supplemented with 10% (v/v) fetal calf serum, 1% penicillin/streptomycin mixture, and 10 μg/ml blasticidin at 37°C in a 5% CO_2 humidified atmosphere. HEK293T cells were maintained in DMEM supplemented with 0.292 g/litre L-glutamine and 10% (v/v) newborn calf serum at 37 °C in a 5% CO_2 humidified atmosphere. Transfection was performed using 1 mg/ml PEI, linear MW-25000. Cells were plated until 60-80% confluent then transfected with 5 μg of required plasmid DNA and PEI, (ratio 1:6 DNA:PEI), diluted in 150 mM NaCl, pH

JPET Fast Forward. Published on September 11, 2012 as DOI: 10.1124/jpet.112.198945
This article has not been copyedited and formatted. The final version may differ from this version.

7.4. After incubation at room temperature for 10 min, the mixture was added to HEK 293T cells. Cells were incubated 24 h then transferred to 96 well plates coated with poly-D-lysine. In all experiments, the total amount of DNA transfected was equalized between constructs by the addition of the empty expression vector pcDNA3.

Generation of Flp-In™ TREx™ 293 cells stably expressing forms of GPR35 **-** To generate Flp-In™ TREx™ 293 cells able to inducibly express human FLAG-GPR35-eYFP, rat FLAG-GPR35-eYFP or mouse FLAG-GPR35-eYFP, the cells were transfected with a mixture containing the desired cDNA in pcDNA5/FRT/TO vector and the pOG44 vector (1:9) using Effectene (Qiagen), according to the manufacturer's instructions. After 48 h, the medium was changed to medium supplemented with 200 μg/ml hygromycin B to initiate selection of stably transfected cells. Following isolation of resistant cells, expression of the appropriate construct from the Flp-In™ TREx™ locus was induced by treatment with up to 100 ng/ml doxycycline for 24 h.

BRET **-** HEK293T cells were co-transfected with the required ortholog of FLAG-GPR35 tagged with eYFP and β-arrestin-2-*Renilla* luciferase 6 (ratio 4:1), using PEI. An additional set of transfections employed only the *Renilla* luciferase construct and empty expression vector pcDNA3From 10 cm dishes, 50,000 cells were seeded per well into poly-D-lysine coated 96 well plates. After 24 h cells were washed twice with Hank's Balanced Salt Solution (pH 7.4), and coelentrazine-h (Promega) was added to a final concentration of 5 μM. Cells were incubated in darkness for 10 min at 37°C before addition of ligands. Cells were incubated a further 5 min at 37°C before reading on a PHERAstar FS reader. The BRET ratio was then calculated as emission

at 530 nm/emission at 485 nm. Net BRET was defined as the 530 nm/485 nm ratio of cells co-expressing the *Renilla* luciferase and eYFP constructs minus the BRET ratio of cells expressing only the *Renilla* luciferase construct in the same experiment. This value was multiplied by 1000 to obtain mBRET units.

Internalization and live cell epifluorescence microscopy - Cells expressing human or rat FLAG-GPR35-eYFP were grown on poly-D-lysine coated coverslips. The coverslips were placed into a microscope chamber containing physiological saline solution (130 mM NaCl, 5 mM KCl, 1 mM $CaCl_2$, 1 mM $MgCl_2$, 20 mM HEPES, and 10 mM D-glucose, pH 7.4). For internalization studies, ligands were added to the microscope chamber and fluorescent images were acquired at 5 min intervals using a spinning disk structured illumination Viva Tome device attached to the bottom port of a Zeiss Axio Observer.Z1 invert microscope (Carl Zeiss). Narrow band 490/20 nm excitation light was reflected through a ×63, oil immersion Plan-Apochromat objective lens to excite eYFP and the resulting emitted light was detected at 536/40 nm using an Axiocam MRm CCD camera (Carl Zeiss).

ArrayScan™ high content analysis of GPR35 internalization Flp-In™ T-Rex™ 293 cells harboring human FLAG-GPR35-eYFP, rat FLAG-GPR35-eYFP or mouse FLAG-GPR35-eYFP were seeded into poly-D-lysine coated clear-view 96 well plates at a density of 60,000 cells per well and treated with up to 100 ng/ml doxycycline to induce receptor construct expression. After 24 h cells were washed twice with HBSS and incubated with ligands for 1 h at 37^{o}C. Cells were then incubated for a further 30 min with ligands and 10μg/ml Hoechst nuclear stain at 37^{o}C. Images were acquired

JPET Fast Forward. Published on September 11, 2012 as DOI: 10.1124/jpet.112.198945
This article has not been copyedited and formatted. The final version may differ from this version.

immediately using a Cellomics ArrayScan™ II high content imager and internalized receptors quantified using a proprietary algorithm designed to identify the number of endosomal recycling compartments per cell.

Inositol phosphate accumulation assays

HEK293T cells were transiently co-transfected with the human, rat, or mouse orthologs of FLAG-GPR35-eYFP and a chimeric G protein (either $G\alpha_{qi}5$ or $G\alpha_{q13}5$) using PEI. After 16-24 h incubation at 37°C, + 5% CO_2, cells were resuspended in IP-One stimulation buffer, (10 mM HEPES, 1 mM $CaCl_2$, 0.5 mM $MgCl_2$, 4.2 mM KCl, 146 mM NaCl, 5.5 mM glucose, 50 mM LiCl, pH7.4) and seeded at 10,000 cells/well in white, solid bottom 384 well plates. Ligands were diluted in IP-One stimulation buffer according to manufacturer's instructions (Cisbio HTRF IP-One Tb kit). Antagonist compounds were pre-incubated with cells for 15 min at 37 ºC prior to addition of agonist. Cells were incubated with agonist for 2 h at 37ºC, before addition of d2-conjugated IP_1 and anti-IP_1 Lumi4™-Tb cryptate diluted in lysis buffer as per manufacturer's instructions. After incubation at room temperature for 1 h, HTRF was measured using a PHERAstar FS plate reader.

Data analysis and curve fitting

All data presented represent mean ± standard error of at least three independent experiments. Data analysis and curve fitting was carried out using the Graphpad Prism software package v5.0b. Concentration-response data were fit to three parameter sigmoidal concentration-response curves. All statistical analysis of curve fit parameters was carried out by independently fitting the data from triplicate

JPET Fast Forward. Published on September 11, 2012 as DOI: 10.1124/jpet.112.198945
This article has not been copyedited and formatted. The final version may differ from this version.

experiments and comparing the resulting curve fit values by t-test or one-way ANOVA as appropriate.

Results

Pamoate is a highly selective but partial agonist for human GPR35 in a β-arrestin-2 recruitment assay

BRET-based GPR35-β-arrestin-2 interaction assays were established in HEK293T cells following co-transfection of species orthologs of FLAG-GPR35-eYFP and β-arrestin-2 *Renilla* luciferase. As reported previously (Jenkins et al., 2010, 2011) zaprinast (**Figure 1**), which in the absence of a clearly defined, high potency endogenous agonist (Milligan, 2011) is often used as a reference ligand at GPR35, produced robust, concentration-dependent BRET signals. Zaprinast was significantly ($p < 0.001$) more potent (pEC_{50} = 7.02 +/- 0.05, mean +/- SEM, n = 7) in producing this effect at rat GPR35 than at the human ortholog (pEC_{50} = 5.30 +/- 0.03, mean +/- SEM, n = 6). Equivalent studies with mouse GPR35 confirmed that zaprinast also acted as an agonist at this ortholog with potency (pEC_{50} = 6.01 +/- 0.06, n = 6) intermediate between the two other species (**Figure 2A**). The anti-asthma medicine and histamine sensitizer cromolyn disodium (**Figure 1**) (Jenkins et al., 2010; Yang et al., 2010) also acted as an agonist with efficacy equal to that of zaprinast at all three species orthologs. In this case ligand potency was lower, but was relatively similar between the human and rat orthologs with pEC_{50} = 4.78 +/- 0.10 (mean +/- SEM, n = 7) at the human receptor, 5.30 +/- 0.03 (n = 3) at rat, and somewhat lower, 4.24 + /- 0.06 (n = 9) at mouse GPR35 (**Figure 2B**). We have also previously reported that whilst pamoate (**Figure 1**) is a relatively high potency (pEC_{50} = 7.28 +/ - 0.07, mean

JPET Fast Forward. Published on September 11, 2012 as DOI: 10.1124/jpet.112.198945
This article has not been copyedited and formatted. The final version may differ from this version.

+/- SEM, n = 7) although partial (E_{max} = 54.8 +/ - 0.8 %) agonist at human GPR35 compared to zaprinast in such BRET-based GPR35-β-arrestin-2 interaction assays (**Figures 2C, 2D**) it has little agonist (**Figure 2C**), or indeed antagonist (Jenkins et al., 2010), activity at rat GPR35. This was also the case when examining mouse GPR35, with only a hint of agonism detected in this assay at concentrations up to 1 x 10^{-5}M (**Figure 2C**). This was somewhat surprising because Zhao et al., (2010) have reported pamoate to have agonist function at mouse GPR35 in a distinct β-arrestin-2 interaction assay.

Pamoate is also highly species ortholog selective in an assay of ligand-induced internalization of GPR35

Because of these differences we also assessed function of these ligands in receptor internalization assays. As well as interacting strongly with β-arrestin-2 in an agonist-dependent manner human GPR35 has been reported to internalize from the surface of cells upon exposure to agonist ligands (Zhao et al., 2010; Jenkins et al., 2011; Deng et al., 2012). Human FLAG-GPR35-eYFP was cloned into the Flp-In™ locus of Flp-In™ TREx™ 293 cells and a pool of cells isolated that were able to express this construct upon addition of the antibiotic doxycycline. Induction of expression resulted in plasma membrane delivery of the receptor (**Figure 3**) and addition of zaprinast (1 x 10^{-5}M) resulted in marked internalization of the eYFP-tagged receptor into punctate intracellular vesicles (**Figure 3**). Similar effects were noted in cells induced to express rat FLAG-GPR35-eYFP (**Figure 3**). Such effects were quantified in cell populations using an ArrayScan™ high content imager. Zaprinast, pEC_{50} = 6.01 +/- 0.07 (**Figure 4A**), cromolyn disodium, pEC_{50} = 5.19 +/-

JPET Fast Forward. Published on September 11, 2012 as DOI: 10.1124/jpet.112.198945
This article has not been copyedited and formatted. The final version may differ from this version.

0.10 (**Figure 4B**) and pamoate, pEC_{50} = 6.86 +/- 0.11 (**Figure 4C**) (each n = 3) all promoted internalization of human FLAG-GPR35-eYFP in a concentration-dependent fashion with EC_{50} values similar to and with the same rank-order of potency (pamoate > zaprinast > cromolyn disodium) (**Figure 4D)** as obtained in the BRET-based β-arrestin-2 interaction assays (**Table 1**). However, when similar studies were performed on equivalent cells able to induce expression of mouse FLAG-GPR35-eYFP, although zaprinast again produced internalization with pEC_{50} = 6.63 +/- 0.13 (**Figure 4A**) similar to that observed in the BRET-based β-arrestin-2 interaction assay, pamoate was completely without effect at concentrations up to 1 x 10^{-4}M (**Figure 4C**) and, although cromolyn disodium did promote internalization of mouse FLAG-GPR35-eYFP at concentrations above 1 x 10^{-5}M, an EC_{50} value could not be estimated accurately (**Figure 4B**). In cells induced to express rat FLAG-GPR35-eYFP zaprinast again promoted internalization of the receptor with pEC_{50} = 7.41 +/- 0.11 (**Figure 4A**), pamoate produced no significant effect at concentrations below 1 x 10^{-5}M (**Figure 4C**) whilst cromolyn disodium produced only a small effect (**Figure 4B**).

Antagonists of GPR35 also display marked species ortholog selectivity

Based on the marked species selectivity of certain agonist ligands we next considered if this might also be true of reported antagonists. CID-2745687 (**Figure 1**) is the only GPR35 antagonist so far detailed in the primary scientific literature (Zhao et al., 2010). Using the BRET-based GPR35-β-arrestin-2 interaction assay and an EC_{80} concentration of zaprinast (2 x 10^{-5}M) as agonist, CID-2745687 behaved as a moderately potent, concentration-dependent antagonist at human GPR35 with pIC_{50} = 6.70 +/ - 0.09 (mean +/- SEM, n = 9) (**Figure 5A**). By contrast, even at 1 x 10^{-4}M

JPET Fast Forward. Published on September 11, 2012 as DOI: 10.1124/jpet.112.198945
This article has not been copyedited and formatted. The final version may differ from this version.

CID-2745687 did not substantially block the agonist action of an EC_{80} concentration of zaprinast (4 x 10^{-6}M) at mouse GPR35 (**Figure 5A**) and a similar inability to antagonize the effect of an EC_{80} concentration of zaprinast (4 x 10^{-7}M) was observed when using rat GPR35 (**Figure 5A**). This again was unexpected as Zhao et al., (2010) have reported CID-2745687 to block effects of zaprinast in a mouse pain model. Equivalent results were obtained when employing cromolyn disodium as agonist. Once again, a concentration-dependent inhibitory activity of CID-2745687 (pIC_{50} = 6.27 +/- 0.08, mean +/- SEM, n = 9) to fully reverse the agonist action of an EC_{80} concentration of cromolyn disodium was observed only at the human ortholog (**Figure 5B**). Although only able to explore the ability to inhibit the agonist action of pamoate at human GPR35, again CID-2745687 did so fully and in a concentration-dependent manner with pIC_{50} = 7.16 +/- 0.12 (mean +/- SEM, n = 9) (**Figure 5C**).

ML-145 (CID-2286812) (**Figure 1**), identified in a β-arrestin-dependent high content screen, has also recently been described as an antagonist of GPR35 (Heynen-Genel et al., 2010). As with CID-2745687, ML-145 fully inhibited the agonist effects of EC_{80} concentrations of each of zaprinast (**Figure 6A**), cromolyn disodium (**Figure 6B**) and pamoate (**Figure 6C**) at human GPR35 in a concentration-dependent manner. Consistent with the reported higher affinity of ML-145 (Heynen-Genel et al., 2010), in each case this ligand displayed higher potency than CID-2745687 (**Table 2**). Once again, however, ML-145 was either without effect (mouse) or displayed only a small and apparently non-competitive inhibitory effect (rat) at the rodent orthologs (**Figure 6A, 6B).**

JPET Fast Forward. Published on September 11, 2012 as DOI: 10.1124/jpet.112.198945
This article has not been copyedited and formatted. The final version may differ from this version.

Both CID-2745687 and ML-145 can also prevent agonist-induced internalization of human GPR35).

Importantly, both CID-2745687 and ML-145 (1 x 10^{-5}M) also fully blocked internalization of human FLAG-GPR35-eYFP in response to varying concentrations of zaprinast, cromolyn disodium and pamoate (**Figure 7A-C**). This was not the case for either CID-2745687 or ML-145 when tested against zaprinast at rat FLAG-GPR35-eYFP (**Figure 7D)** whilst at mouse FLAG-GPR35-eYFP, although ML-145 was without effect on the potency or effect of zaprinast (**Figure 7E**), at 1 x 10^{-5}M CID-2745687 consistently produced a modest but not statistically significant decrease in potency but not maximal effect of zaprinast (**Figure 7E)**. To explore this more fully, the ability of varying concentrations of ML-145 or CID-2745687 to prevent internalization of either the human or mouse orthologs of GPR35 in response to an EC_{80} concentration of zaprinast was assessed. Here, both ML-145 (**Figure 8A**) and CID-2745687 (**Figure 8B**) were effective inhibitors of zaprinast at the human ortholog but neither produced a substantial effect at the mouse ortholog (**Figure 8C, 8D**). Equivalent results for both ML-145 (**Figures 8A, 8C**) and CID-2745687 (**Figure 8B and 8D**) were produced when EC_{80} concentrations of either cromolyn disodium (at both human and mouse GPR35) or pamoate (only at the human ortholog) were employed.

Ligand selectivity at GPR35 orthologs is also observed in G protein-dependent assays

Each of the assays described above is G protein-independent. GPR35 has been indicated to interact, however, with both pertussis toxin-sensitive G_i family G proteins

JPET Fast Forward. Published on September 11, 2012 as DOI: 10.1124/jpet.112.198945
This article has not been copyedited and formatted. The final version may differ from this version.

(Wang et al., 2006) and with the non pertussis toxin-sensitive G protein $G\alpha_{13}$ (Jenkins et al., 2011). We took advantage of this to establish inositol monophosphate (IP_1) accumulation assays following transfection of HEK293T cells with an ortholog of FLAG-GPR35-eYFP along with either chimeric $G_{q\text{-}i}(5)$ or $G_{q\text{-}13}(5)$ $G\alpha$ subunits (Milligan and Kostenis, 2006; Kostenis et al., 2005). A positive control for IP_1 production was provided by transfecting cells with the muscarinic M_3 acetylcholine receptor and adding the synthetic acetylcholine mimetic carbachol (1×10^{-3}M) (**Figure 9A**) as this receptor is known to couple effectively to inositol phosphate production and the subsequent elevation of $[Ca^{2+}]_i$. In preliminary experiments we demonstrated that zaprinast (1×10^{-5}M) increased levels of IP_1 when human FLAG-GPR35-eYFP and either of these G protein chimeras were co-expressed (**Figure 9A**). Such an effect of zaprinast was not observed either when human FLAG-GPR35-eYFP was co-expressed with full length G_q (**not shown**) or when either of the G protein chimeras was expressed without GPR35 (**Figure 9A**). Interestingly, in the absence of zaprinast co-expression of human FLAG-GPR35-eYFP along with either of the G protein chimeras resulted in greater accumulation of IP_1 than in the absence of the receptor, potentially consistent with a level of receptor constitutive activity in this assay (**Figure 9A**). Subsequently we expressed human FLAG-GPR35-eYFP along with either $G_{q\text{-}i}(5)$ or $G_{q\text{-}13}(5)$ and explored the concentration-dependence for zaprinast induction of IP_1 generation (**Figure 9B**). Zaprinast was significantly more potent (pEC_{50} = 6.98 +/- 0.14 ($G_{q\text{-}i}(5)$), = 7.08 +/- 0.12 ($G_{q\text{-}13}(5)$) (n = 3) in these assays than in either of the non G protein-dependent assays, but was not different between the two chimeric G proteins. Similar results were obtained when using rat FLAG-GPR35-eYFP except that, as in the other assays, zaprinast was significantly

more potent (pEC_{50} = 8.47 +/- 0.09 (G_q-$_i$(5), and 8.51 +/- 0.05 (G_q-$_{13}$(5)) than at the human ortholog (**Figure 9C**). When using mouse FLAG-GPR35-eYFP the equivalent values were pEC_{50} = 8.32 +/- 0.24 (G_q-$_i$(5)), and 7.80 +/- 0.04 (G_q-$_{13}$(5)) (**Figure 9C**). Subsequent studies predominantly employed the G_q-$_{13}$(5) chimera. As in the β-arrestin-2 interaction assays, cromolyn disodium was as efficacious as zaprinast and again more potent in this assay (pEC_{50} = 6.32 at human, 5.82 at rat and 5.55 at mouse) (**Figure 9C**). The enhanced potency of ligands in this assay allowed re-assessment of potential agonism of pamoate at the rodent orthologs of GPR35 (**Figure 9C**). At human GPR35 pamoate displayed high potency (pEC_{50} = 8.44 +/ - 0.13) and was some 30 fold more potent than zaprinast (**Figure 9C**). Interestingly, in this assay, pamoate acted as a full agonist with respect to zaprinast (**Figure 9C**). Despite this, at mouse GPR35 pamoate remained virtually inactive, with no significant agonist function uncovered at concentrations below 1 x 10^{-5}M (**Figure 9C**). As such, pamoate displays at least 3000 fold selectivity for human over murine GPR35 in this assay. At the rat ortholog pamoate did display some activity (pEC_{50} = 6.15 +/ - 0.18) (**Figure 9C**) but remained some 200 fold less potent than at human GPR35.

As anticipated from the other assays, ML-145 inhibited the effect of EC_{80} concentrations of zaprinast (3 x 10^{-7}M), cromolyn disodium (3x 10^{-6}M) and pamoate (1 x 10^{-8}M) at human GPR35 in the IP_1 accumulation assays with pIC_{50} close to 7.4 in these conditions (**Figure 10A**). Furthermore, ML-145 also decreased basal IP_1 production in a concentration-dependent manner (**Figure 10A**), consistent with this ligand behaving as an inverse agonist and suppressing the constitutive activity of human GPR35. By contrast, ML-145 displayed little capacity to inhibit the agonist action of an EC_{80} concentration of zaprinast at either mouse or rat GPR35 in this assay

JPET Fast Forward. Published on September 11, 2012 as DOI: 10.1124/jpet.112.198945
This article has not been copyedited and formatted. The final version may differ from this version.

(**Figure 10A**). Although necessary to employ pamoate at 3 x 10^{-6}M to generate a substantial signal via rat GPR35, again ML-145 was entirely without effect at concentrations up to 1 x 10^{-5}M (**Figure 10A**). CID-2745687 also inhibited the effect of each of zaprinast, cromolyn disodium and pamoate at human GPR35 in a concentration-dependent manner but was more than 10 fold less potent than ML-145 (**Figure 10B**). As for ML-145, CID-2745687 also acted as an inverse agonist, able to reduce basal IP_1 generation in a concentration-dependent manner (**Figure 10B**). As noted for ML-145, CID-2745687 was without significant effect at either rat or mouse GPR35 in these assays (**Figure 10B**).

ML-145 is a competitive antagonist at human GPR35

To define the mode of action of ML-145 at human GPR35 we returned to the BRET-based β-arrestin-2 interaction assay and performed a series of agonist concentration-response curves to zaprinast (**Figure 11A**), cromolyn disodium (**Figure 11B**) and pamoate (**Figure 11C**) in the presence of concentrations of ML-145 ranging from 1-50 nM. In all cases global analysis of the data was consistent with ML-145 acting as a competitive and surmountable antagonist, although the relatively low potency of cromolyn disodium meant that sufficient agonist could not be used to fully overcome the effect of the highest concentration of ML-145 employed. Such studies produced estimates of the pA_2 for ML-145 between 8.67-8.83 (1.48 - 2.13 x 10^{-9}M).

CID-2745687 inhibits the action of agonists at human GPR35 by distinct mechanisms

To assess if CID-2745687 also acted as a competitive antagonist the ability of a range of concentrations of this ligand to alter the concentration-response curves of each of zaprinast, cromolyn disodium and pamoate was also examined at human GPR35. For both zaprinast (**Figure 11D**) and cromolyn disodium (**Figure 11E**) such studies produced surmountable shifts in the potency of the agonist to higher concentrations. Global fit analyses of such curves were also consistent with a competitive mode of antagonism with pA_2 affinity values for CID-2745687 of 7.7-7.8 (1.6 -1.9 x 10^{-8}M) and slope factor close to 1.0. By contrast, equivalent studies with pamoate produced very different results (**Figure 11F**). Increasing concentrations of CID-2745687 had little effect on the EC_{50} of pamoate but rather decreased the maximal effect of the agonist, indicative of a non-competitive mode of action.

Consistent with the observations that both zaprinast and cromolyn disodium were antagonized competitively by each of CID-2745687 and ML-145 and are both full agonists in the β-arrestin-2 interaction assay, addition of a series of sub-maximally effective concentrations of cromolyn disodium did not alter the observed EC_{50} of zaprinast at human GPR35 (**Figure 12)**, suggesting the two agonists share a common or overlapping binding site (Jenkins et al., 2011).

Discussion

In recent times the poorly characterized GPCR GPR35 has been suggested to be a potential therapeutic target in areas ranging from diabetes, cardiovascular disease and inflammation to pain (Milligan, 2011; MacKenzie et al., 2011). In part, this has been based simply on the expression patterns of GPR35. However, as a GPR35 knock-out line of mice has been reported to have markedly elevated blood pressure

(Min et al., 2010), whilst blockade of acetic acid-induced writhing in mice has been shown to be limited by certain ligands, including pamoate (Zhao et al., 2010) and zaprinast (Cosi et al., 2011), that are reported to have agonist potency at GPR35, there are a developing number of supporting physiological studies. Despite this, to date only the studies of Min et al., (2010) have employed GPR35 knock-out animals. This means that detailed pharmacological analysis of proposed ligands at GPR35 must be performed and understood with multiple species orthologs of the receptor prior to linking other potential physiological functions to regulation of GPR35. Many of the ligands reported to have agonist action at GPR35 display modest potency (Jenkins et al., 2010; Yang et al., 2010, 2012; Deng and Fang, 2012; Deng et al., 2011, 2012; Hu et al., 2012) and frequently are also known to have other molecular targets. For example, despite both kynurenic acid (Wang et al., 2006) and lysophosphatidic acid (Oka et al., 2010) being proposed as endogenous activators of GPR35, the synthetic ligand zaprinast has become the standard reference agonist. Zaprinast, however, is better appreciated as an inhibitor of cGMP phosphodiesterases (Taniguchi et al., 2006) and other recently reported GPR35 agonists are generally either very simple molecules with modest potency/affinity and known activity at multiple other targets (Yang et al., 2010, 2012; Deng and Fang, 2012; Deng et al., 2012; Hu et al., 2012) or were identified via screens of libraries of known therapeutic ligands (Jenkins et al., 2010). As such, the identification of pamoate as a relatively potent GPR35 agonist (Zhao et al., 2010; Jenkins et al., 2010) potentially offers a more useful tool.

Potential species ortholog selectivity of ligands is a major issue for target validation and candidate selection in the drug discovery arena and even one of the initial reports of the activity of pamoate as a GPR35 agonist noted that although

identified in a screen against human GPR35 this was not replicated when rat GPR35 was the target (Jenkins et al., 2010). Furthermore, in the current studies we have extended such studies to demonstrate that pamoate has no substantial agonist action at mouse GPR35. Observations of marked variation in pharmacology of species orthologs of GPCRs are well known but are of particular relevance in the early stages of receptor characterization. For example, the differences in ligand affinity at orthologs of the histamine H4 receptor (Liu et al., 2001) even led to suggestions that their might be yet further receptors for histamine and further detailed pharmacological characterization of various orthologs of this receptor (Lim et al., 2010, Schnell et al., 2011), whilst the development of early generation β_3-adrenoceptor selective agonists was severely compromised by, at that time unappreciated, ortholog selectivity (de Souza and Burkey, 2001, Arch, 2008).

The recent reports of the identification of a pair of chemically distinct GPR35 antagonists with nanomolar potency at this receptor (Zhao et al., 2010; Heynen-Genel et al., 2010) also potentially offered an excellent avenue to explore the biology and physiological function of GPR35. However, based on the issues with species selectivity of agonists at this receptor we wished to explore both the mode of action and any potential species selectivity of these ligands. Although we have been able to confirm that CID-2745687 and ML-145 are indeed high affinity antagonists, and indeed inverse agonists, at human GPR35 they are both close to inactive at each of the rat and mouse orthologs. This means that they can be of no use in assessing the role of GPR35 in either cell or *in vivo* models based on these species. It is, therefore, most likely that the reported capacity of CID-2745687 to block pamoate-induced effects on writhing in a mouse model of pain (Zhao et al., 2010) reflects non GPR35-mediated

mechanisms for both the purported agonist and antagonist, although what the molecular target was in these studies remains unclear. Despite this, the activity of the antagonist ligands at human GPR35 should be of considerable use to assess, for example, if the reported ability of kynurenic acid to enhance interactions of human leukocytes with vascular endothelium under flow conditions (Barth et al., 2009) is truly a GPR35-mediated effect. Although short hairpin RNA-mediated silencing of GPR35 was certainly consistent with this, the high potency of kynurenic acid reported in experiments employing human umbilical vein endothelial cells (Barth et al., 2009) was surprising given the low potency of this ligand noted at human GPR35 in *in vitro* assays (Jenkins et al., 2011; Deng et al., 2012).

ML-145 acted as a competitive and surmountable antagonist against each of the three selected agonists at human GPR35 and this was also true for CID-2745687 against zaprinast and cromolyn disodium. Consistent with this, additivity studies using combinations of zaprinast and cromolyn disodium suggested that these two agonists bind to a common site. By contrast, CID-2745687 displayed non-competitive inhibition of the effect of pamoate, suggesting that pamoate, which was clearly a partial agonist at human GPR35 in β-arrestin-2 interaction assays, may bind in a distinct manner. Further, detailed analysis will be required to define this more fully. As the endogenous ligand(s) that activate GPR35 remain to be fully defined then definition of the orthosteric binding pocket is challenging. However, previous mutagenesis studies have suggested a key role of arginine 3.36 (position 108 in the short isoform of human GPR35) (Milligan, 2011) (**Figure 13**). Many of the reported GPR35 agonists, including the purported endogenous acid kynurenic acid and pamoate, have a carboxylate moiety that could provide an ionic interaction with the

side chain of this residue. Alignment of the human, mouse and rat orthologs of GPR35 shows the conversation of this residue (**Figure 13**). However, as GPR35 is distant phylogenetically from any of the GPCRs for which atomic level crystal stuctures are currently available efforts to employ homology modelling for example to understand the variations in pharmacology between species remain extremely challenging.

A potentially important point is that many of the efforts to identify novel GPR35 agonists have been based on G protein-independent assays. In part this reflects that in both academic and industrial settings GPCR agonist screens based on interactions with a β-arrestin have become more dominant in recent times (Hamdan et al., 2005). This is due to a combination of the relative ease of performing such studies and the argument that they are more 'universal' (Verkaar et al., 2008). In the case of poorly characterized GPCRs this has an abiding attraction if the G protein-coupling profile of the receptor is unknown. Specifically in relation to GPR35 various studies have indicated roles for both pertussis toxin-sensitive G_i-family G proteins (Wang et al., 2006; Oshiro et al., 2008; Barth et al., 2009) and $G\alpha_{13}$ (Jenkins et al., 2010, 2011) in signal transduction and it was certainly possible that the structure-activity relationship of certain GPR35 agonists might be distinct in a G protein-dependent assay when compared to a G protein-independent assay, a feature usually described as bias (DeWire et al., 2007; Luttrell and Kenakin, 2011). Chimeric G protein α subunits, in which the extreme C-terminal receptor recognition element of one G proteins is introduced into the sequence of a second G protein in which the effector recognition element provides an easy to automate functional assay (Coward et al., 1999, Milligan and Kostenis, 2006), have been a mainstay of industrial level GPCR-

ligand screening programmes (Milligan and Rees, 1999, Milligan and Kostenis, 2006), particularly in allowing linkage to the elevation of intracellular Ca^{2+} (Emkey and Rankl, 2009). Although prior to these studies there was limited available information on either if chimeric G proteins could be employed to studt GPR35 or on potential ligand bias we now show clearly that in assays in which chimeric G proteins are used to couple the species orthologs of GPR35 to the production of inositol phosphates, the same basic pharmacology is observed as in the β-arrestin-2 recruitment assay, in that although pamoate is a potent activator of human GPR35 this is not the case at either the rat or mouse orthologs. Although the relatively high potency of GPR35 ligands in the inositol phosphate assays and the apparent full agonism of pamoate at the human receptor was useful in allowing detailed analysis of the selectivity of ligands between the species orthologs, these features may reflect receptor and G protein reserve as expression levels in such transient assays were not clearly defined. Furthermore, although restricted to studies on the human ortholog, it is noteworthy that Deng et al., (2012) recently noted that the rank-order of potency of a group of previously characterized GPR35 agonists including pamoate, zaprinast and cromolyn disodium was the same in both a GPR35-β-arrestin interaction assay and when using dynamic mass redistribution, a 'label-free' approach that integrates signals from all G protein-mediated pathways (Schroder et al., 2011), in human HT-29 cells that express this receptor endogenously. Overall these sets of studies suggest that at least for the ligands used herein it is unlikely that marked bias exists.

Although it is also possible that non-receptor accessory proteins might alter the pharmacology of GPR35 in a species-dependent manner, the current studies re-emphasize the need to perform standard but insightful pharmacological analyses to

fully understand both the potential and the potential limitations of novel ligands identified via various screens and their detailed mode of action. The current studies define that despite their high affinity at human GPR35 neither CID-2745687 nor ML-145 are useful pharmacological antagonists to probe the functions of GPR35 in either mouse or rat models of physiology and disease and that pamoate is not a high potency agonist at rodent orthologs of this receptor.

Authorship contribution

Participated in research design: Jenkins, Harries, Lappin, Mackenzie, Neetoo-Isseljee, Southern, McIver, Taylor, Nicklin, Milligan
Conducted experiments: Jenkins, Harries, Lappin, Mackenzie, Neetoo-Isseljee.
Contributed new reagents or analytic tools: McIver, Southern, Taylor
Performed data analysis: Jenkins, Harries, Lappin, Mackenzie, Nicklin, Milligan
Wrote or contributed to the writing of the manuscript: Milligan with assistance from all other authors.

References

Arch JR (2008) The discovery of drugs for obesity, the metabolic effects of leptin and variable receptor pharmacology: perspectives from beta3-adrenoceptor agonists. *Naunyn Schmiedebergs Arch Pharmacol* **378**: 225-240.

Barth M, Ahluwalia N, Anderson TJ, Hardy GJ, Sinha S, Alvarez-Cardona JA, Pruitt IE, Rhee EP, Colvin RA, and Gerszten RE (2009) Kynurenic acid triggers firm arrest of leukocytes to vascular endothelium under flow conditions. *J Biol Chem* **284**: 19189-19195.

Cosi C, Mannaioni G, Cozzi A, Carla V, Sili M, Cavone L, Maratea D, and Moroni F (2011) G-protein coupled receptor 35 (GPR35) activation and inflammatory pain: Studies on the antinociceptive effects of kynurenic acid and zaprinast. *Neuropharmacol* **60**: 1227-1231.

Coward P, Chan SD, Wada HG, Humphries GM, and Conklin BR (1999) Chimeric G proteins allow a high-throughput signaling assay of Gi-coupled receptors. *Anal Biochem* **270**: 242-248.

Deng H, and Fang Y (2012) Aspirin metabolites are GPR35 agonists. *Naunyn Schmiedebergs Arch Pharmacol* **385**: 729-737.

Deng H, Hu H, and Fang Y (2011) Tyrphostin analogs are GPR35 agonists. *FEBS Lett* **585**:1957-1962.

Deng H, Hu H, and Fang Y (2012) Multiple tyrosine metabolites are GPR35 agonists. *Sci Rep* **2**:373.

de Souza CJ, Burkey BF (2001) Beta 3-adrenoceptor agonists as anti-diabetic and anti-obesity drugs in humans. *Curr Pharm Des* **7:** 1433-1449.

DeWire SM, Ahn S, Lefkowitz RJ, and Shenoy SK (2007) Beta-arrestins and cell signaling. *Annu Rev Physiol* **69**: 483-510.

Emkey R, and Rankl NB (2009) Screening G protein-coupled receptors: measurement of intracellular calcium using the fluorometric imaging plate reader. *Methods Mol Biol* **565**:145-158.

Hamdan FF, Audet M, Garneau P, Pelletier J, and Bouvier M (2005). High-throughput screening of G protein-coupled receptor antagonists using a bioluminescence resonance energy transfer 1-based beta-arrestin2 recruitment assay. *J Biomol Screen* **10**: 463-475.

Heynen-Genel S, Dahl R, Shi S, Sauer M, Hariharan S, Sergienko E, Dad S, Chung TDY, Stonich D, Su Y, Caron M, Zhao P, Abood ME, and Barak LS. (2010) Selective GPR35 Antagonists - Probes 1 & 2. Probe Reports from the NIH Molecular Libraries Program [Internet]. Bethesda (MD): National Center for Biotechnology Information

(US); 2010-. 2010 Feb 28 [updated 2010 Oct 4]

Hu H, Deng H, and Fang Y (2012) Label-free phenotypic profiling identified D-luciferin as a GPR35 agonist. *PLoS One* **7**: e34934.

Jenkins L, Alvarez-Curto E, Campbell K, de Munnik S, Canals M, Schlyer S, and Milligan G (2011) Agonist activation of the G protein-coupled receptor GPR35 involves transmembrane domain III and is transduced via Galpha and beta-arrestin-2. *Br J Pharmacol* **162**: 733-748.

Jenkins L, Brea J, Smith NJ, Hudson BD, Reilly G, Bryant NJ, Castro M, Loza MI, and Milligan G (2010) Identification of novel species-selective agonists of the G-protein-coupled receptor GPR35 that promote recruitment of beta-arrestin-2 and activate Galpha13. *Biochem J* **432**: 451-459.

Kostenis E, Waelbroeck M, and Milligan G (2005) Techniques: promiscuous Galpha proteins in basic research and drug discovery. *Trends Pharmacol Sci* **26**: 595-602.

Lim HD, de Graaf C, Jiang W, Sadek P, McGovern PM, Istyastono EP, Bakker RA, de Esch IJ, Thurmond RL, Leurs R (2010) Molecular determinants of ligand binding to H4R species variants. *Mol Pharmacol* **77:** 734-743.

Liu C, Wilson SJ, Kuei C, Lovenberg TW (2001) Comparison of human, mouse, rat, and guinea pig histamine H4 receptors reveals substantial pharmacological species variation. *J Pharmacol Exp Ther* **299**: 121-130.

Luttrell LM, and Kenakin TP (2011) Refining efficacy: allosterism and bias in G protein-coupled receptor signaling. *Methods Mol Biol* **756**: 3-35.

MacKenzie AE, Lappin JE, Taylor DL, Nicklin SA, and Milligan G (2011) GPR35 as a novel therapeutic target. *Front. Endocrin. Molecular and Structural Endocrinology* **2**: 68.

Milligan G (2011) Orthologue selectivity and ligand bias: translating the pharmacology of GPR35. *Trends Pharmacol Sci* **32**: 317-325.

Milligan G, and Kostenis E (2006) Heterotrimeric G-proteins: a short history. *Br J Pharmacol* **147** Suppl 1:S46-55.

Milligan G, and Rees S (1999) Chimaeric G alpha proteins: their potential use in drug discovery. *Trends Pharmacol Sci* **20:** 118-124.

Min KD, Asakura M, Liao Y, Nakamaru K, Okazaki H, Takahashi T, Fujimoto K, Ito S, Takahashi A, Asanuma H, Yamazaki S, Minamino T, Sanada S, Seguchi O, Nakano A, Ando Y, Otsuka T, Furukawa H, Isomura T, Takashima S, Mochizuki N, and Kitakaze M (2010) Identification of genes related to heart failure using global

gene expression profiling of human failing myocardium. *Biochem Biophys Res Commun* **393**: 55-60.

Ohshiro H, Tonai-Kachi H, and Ichikawa K (2008) GPR35 is a functional receptor in rat dorsal root ganglion neurons. *Biochem Biophys Res Commun* **365**: 344-348.

Oka S, Ota R, Shima M, Yamashita A, and Sugiura T (2010) GPR35 is a novel lysophosphatidic acid receptor. *Biochem Biophys Res Commun* **395**: 232-237.

Schnell D, Brunskole I, Ladova K, Schneider EH, Igel P, Dove S, Buschauer A, and Seifert R (2011) Expression and functional properties of canine, rat, and murine histamine H4 receptors in Sf9 insect cells. *Naunyn Schmiedebergs Arch Pharmacol* **383**: 457-470.

Schroder R, Schmidt J, Blattermann S, Peters L, Janssen N, Grundmann M, Seemann W, Kaufel D, Merten N, Drewke C, Gomeza J, Milligan G, Mohr K, and Kostenis E (2011) Applying label-free dynamic mass redistribution technology to frame signaling of G protein-coupled receptors non-invasively in living cells. *Nature Protocols* **6**: 1748-1760.

Taniguchi Y, Tonai-Kachi H, and Shinjo, K (2006). Zaprinast, a well-known cyclic guanosine monophosphate-specific phosphodiesterase inhibitor, is an agonist for GPR35. *FEBS Lett* **580**: 5003-5008.

Verkaar F, van Rosmalen JW, Blomenröhr M, van Koppen CJ, Blankesteijn WM, Smits JF, and Zaman GJ (2008) G protein-independent cell-based assays for drug discovery on seven-transmembrane receptors. *Biotechnol Annu Rev* **14**:253-274.

Wang J, Simonavicius N, Wu X, Swaminath G, Reagan J, Tian H, and Ling L (2006) Kynurenic acid as a ligand for orphan G protein-coupled receptor GPR35. *J Biol Chem* **281**: 22021-22028.

Yang Y, Lu JY, Wu X, Summer S, Whoriskey J, Saris C, and Reagan JD (2010) G-protein-coupled receptor 35 is a target of the asthma drugs cromolyn disodium and nedocromil sodium. *Pharmacology* **86**:1-5.

Yang Y, Fu A, Wu X, and Reagan JD (2012) GPR35 is a target of the loop diuretic drugs bumetanide and furosemide. *Pharmacology* **89**:13-17.

Zhao P, Sharir H, Kapur A, Cowan A, Geller EB, Adler MW, Seltzman HH, Reggio PH, Heynen-Genel S, Sauer M, Chung TD, Bai Y, Chen W, Caron MG, Barak LS, and Abood ME (2010). Targeting of the orphan receptor GPR35 by pamoic acid: a potent activator of extracellular signal-regulated kinase and beta-arrestin2 with antinociceptive activity. *Mol Pharmacol* **78**: 560-568.

Footnotes

AEM thanks the Biotechnology and Biosciences Research Council and JEL the British Heart Foundation for studentship support.

JPET Fast Forward. Published on September 11, 2012 as DOI: 10.1124/jpet.112.198945
This article has not been copyedited and formatted. The final version may differ from this version.

Figure Legends

Figure 1 Structure of ligands studied

Structures of the three agonist ligands, zaprinast, cromolyn disodium and pamoate, as well as the two previously reported antagonists, methyl-5-[(tert-butylcarbamothioylhydrazinylidene)methyl]-1-(2,4-difluorophenyl)pyrazole-4-carboxylate (CID-2745687) and 2-hydroxy-4-[4-(5*Z*)-5-[(*E*)-2-methyl-3-phenylprop-2-enylidene]-4-oxo-2-sulfanylidene-1,3-thiazolidin-3-yl]butanoylamino]benzoic acid (ML-145, CID-2286812), are shown.

Figure 2 Pamoate is a GPR35 partial agonist with high selectivity for the human ortholog

(**A-C**) BRET-based GPR35-β-arrestin-2 interaction assays were performed in HEK293T cells using human (**circles**), mouse (**squares**) or rat (**triangles**) FLAG-GPR35-eYFP constructs. The effects of varying concentrations of zaprinast (**A**), cromolyn disodium (**B**) and pamoate (**C**) were assessed. **D**. The potency and relative efficacy of these ligands at human GPR35 is displayed. Data are representative of at least 6 different experiments.

Figure 3 Zaprinast promotes internalization of both human and rat GPR35-eYFP

Flp-In^{TM} TREx^{TM} 293 cells able to express either human (**upper panels**) or rat (**lower panels**) FLAG-GPR35-eYFP upon addition of doxycycline were induced with this antibiotic for 24 hours. Such cells were then exposed to vehicle (**left hand panels**) or

zaprinast (1 x 10^{-5}M) (**right hand panels**) for 30 min prior to imaging. A scale bar is indicated.

Figure 4 Pamoate-mediated internalization of GPR35 is restricted to the human ortholog

(**A-C**) Flp-In™ TREx™ 293 cells able to express human (**circles**), mouse (**squares**) or rat (**triangles**) FLAG-GPR35-eYFP constructs upon addition of doxycycline were induced with this antibiotic for 24 hours. The capacity of varying concentrations of zaprinast (**A**), cromolyn disodium (**B)** or pamoate (**C)** to promote internalization of the receptor constructs was then assessed and quantified using an ArrayScan™ high content imager. **D**. The potency and relative efficacy of these ligands at human GPR35 is displayed. Data are representative of at least 6 different experiments.

Figure 5 CID-2745687 is a potent antagonist in β-arrestin-2 interaction assays only at human GPR35

BRET-based GPR35-β-arrestin-2 interaction assays as in Figure 1 were performed using human (**circles**), mouse (**squares**) or rat (**triangles**) FLAG-GPR35-eYFP. In each case an EC_{80} concentration of zaprinast (**A**), cromolyn disodium (**B**) or pamoate (only at human GPR35) (**C**) was added along with varying concentrations of CID-2745687. In (**D**) the effectiveness of CID-2745687 against each agonist at human GPR35 is compared directly.

Figure 6 ML-145 is also a highly selective human GPR35 antagonist in β-arrestin-2 interaction assays

JPET Fast Forward. Published on September 11, 2012 as DOI: 10.1124/jpet.112.198945
This article has not been copyedited and formatted. The final version may differ from this version.

Experiments were conducted as in Figure 4 except that ML-145 replaced CID-2745687. (**A**) zaprinast, (**B**) cromolyn disodium, (**C**) pamoate. In (**D**) the effectiveness of ML-145 against each agonist at human GPR35 is compared directly.

Figure 7 CID-2745687 and ML-145 both block agonist-mediated internalization of human but not of rodent forms of GPR35

The ability of varying concentrations of zaprinast (**A**), cromolyn disodium (**B**) and pamoate (**C**) (**filled circles**) to promote internalization of human GPR35-eYFP and the capacity of either CID-2745687 (**open circles**) or ML-145 (**triangles**) (1×10^{-5}M) to prevent this was assessed via high content imaging using an ArrayScan™ high content imager. In equivalent studies the capacity of varying concentrations of zaprinast to cause internalization of rat (**D**) and mouse (**E**) GPR35-eYFP and any capacity of either CID-2745687 and ML-145 (1×10^{-5}M) to prevent this was assessed.

Figure 8 CID-2745687 and ML-145 block agonist-mediated internalization of human GPR35 in a concentration-dependent fashion

Experiments akin to those of Figure 7 examined the ability of varying concentrations of ML-145 (**A, C**) or CID-2745687 **(B, D)** to prevent internalization of human (**A, B**) or mouse (**C, D**) GPR35 promoted by an EC_{80} concentration of the identified agonist ligands.

Figure 9 GPR35 stimulates IP_1 accumulation when co-expressed with suitable chimeric G protein α subunits

JPET Fast Forward. Published on September 11, 2012 as DOI: 10.1124/jpet.112.198945
This article has not been copyedited and formatted. The final version may differ from this version.

HEK293T cells were transfected with or without human FLAG-GPR35-eYFP alongside either $G_{q-i}(5)$ or $G_{q-13}(5)$ Gα subunits (**A**). Basal (**open bars**) IP_1 accumulation and effects of zaprinast (1×10^{-5}M) on this (**filled bars**) were measured. A positive control was provided following transfection of the M_3 muscarinic acetylcholine receptor and addition of the agonist carbachol (1×10^{-3}M). (**B**) Following co-transfection of human FLAG-GPR35-eYFP along with either $G_{q-i}(5)$ (**circles**) or $G_{q-13}(5)$ (**squares**) Gα subunits the effect of various concentrations of zaprinast were assessed. (**C**) Following transfection of human (**circles**), mouse (**squares**) or rat (**triangles**) FLAG-GPR35-eYFP along with $G_{q-13}(5)$ the ability of varying concentrations of zaprinast (**left**), pamoate (**middle**) or cromolyn disodium (**right**) to promote IP_1 accumulation was assessed.

Figure 10 CID-2745687 and ML-145 block both constitutive and agonist-mediated IP_1 accumulation only at the human ortholog of GPR35

The capacity of varying concentrations of ML-145 (**A**) or CID-2745687 (**B**) to limit IP_1 accumulation in response to EC_{80} concentrations of zaprinast (**left hand panels**), pamoate (**centre**) or cromolyn (**right hand panels**) was assessed in cells transfected to express the noted ortholog of FLAG-GPR35-eYFP along with $G_{q-13}(5)$. Note the marked reduction of IP_1 below basal levels (defined as 0 % on y-axis), indicative of inverse agonism, produced by higher concentrations of each of ML-145 (**A**) and CID-2745687 (**B**) at the human ortholog.

Figure 11 ML-145 is a competitive antagonist at human GPR35 whilst the nature of antagonism by CID-2745687 GPR35 depends on the identity of the agonist

JPET Fast Forward. Published on September 11, 2012 as DOI: 10.1124/jpet.112.198945
This article has not been copyedited and formatted. The final version may differ from this version.

BRET-based GPR35-β-arrestin-2 interaction assays were performed in HEK293T cells as in Figure 1 using human FLAG-GPR35-eYFP. The effects of varying concentrations of ML-145 (**A-C**) or CID-2745687 **(D-F)** on concentration-response curves to zaprinast (**A, D**), cromolyn disodium (**B, E**) and pamoate (**C, F**) are shown in representative experiments.

Figure 12 Zaprinast and cromolyn disodium likely share a common binding site on human GPR35

BRET-based GPR35-β-arrestin-2 interaction assays were performed in HEK293T cells as in Figure 10 using human FLAG-GPR35-eYFP. Concentration-response curves to zaprinast were performed in the presence of a range of sub-maximally effective concentrations of cromolyn disodium. The EC_{50} of zaprinast was unaffected by the co-presence of cromolyn disodium.

Figure 13 Sequence alignment of human, mouse and rat orthologs of GPR35

The sequence of the short isoform of human GPR35 is aligned with the mouse and rat orthologs. Asterisks indicate amino acid identity across these orthologs whilst colons indicate conservative and full stops semi-conservative substitutions between species. Potential transmembrane domains are boxed, The 'DRY' domain and the 'NPXXY' region (light shading), two defining sequence elements of rhodopsin-like, class A GPCRs are highlighted, as are arginine (R) 3.36 and tyrosine (Y) 3.32 (dark shading), mutation of either of these residues to alanine (Jenkins et al., 2011) eliminates the function of all GPR35 agonists for which this has been assessed (MacKenzie et al., 2011). As such these residues likely contribute to the ligand binding pocket.

JPET Fast Forward. Published on September 11, 2012 as DOI: 10.1124/jpet.112.198945
This article has not been copyedited and formatted. The final version may differ from this version.

Tables

Table 1 Comparison of the potency of agonist ligands at human GPR35

Ligand	β-arrestin-2 recruitment (pEC_{50} mean +/- SEM)	Internalization (pEC_{50} mean +/- SEM)
Zaprinast	5.30 +/ - 0.03	6.01 +/- 0.07
Cromolyn disodium	4.78 +/ -0.10	5.19 +/- 0.10
Pamoate	7.28 + / - 0.07 *	6.86 +/- 0.11 *

The potency of ligands at human GPR35 are compared in BRET-based β-arrestin-2 recruitment and receptor internalization assays. * partial agonist when compared to zaprinast.

JPET Fast Forward. Published on September 11, 2012 as DOI: 10.1124/jpet.112.198945
This article has not been copyedited and formatted. The final version may differ from this version.

Table 2 ML-145 displays greater potency as an antagonist at human GPR35 than CID-2745687

Agonist	Antagonist (pIC_{50}, mean +/- SEM) ML-145
Zaprinast	7.57 +/- 0.07
Cromolyn disodium	7.65 +/ 0.07
Pamoate	8.08 +/- 0.12
	CID-2745687
Zaprinast	6.70 +/- 0.09
Cromolyn disodium	6.27 +/ - 0.08
Pamoate	7.16 +/- 0.12

Human GPR35-β-arrestin 2 interaction assays were conducted using EC_{80} amounts of the indicated agonists and varying concentrations of either ML-145 or CID-2745687. In all cases a maximally effective concentration of either antagonist ligand was able to fully reverse the effects of the agonist ligand. Data are means +/- SEM from 9 independent experiments.

Figure 1

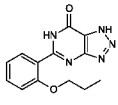

Zaprinast

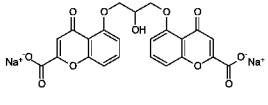

Cromolyn Disodium

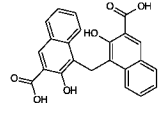

Pamoate

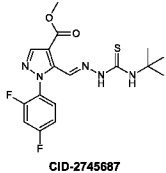

CID-2745687

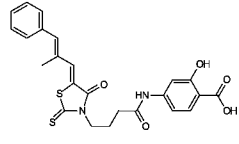

ML-145

Figure 2

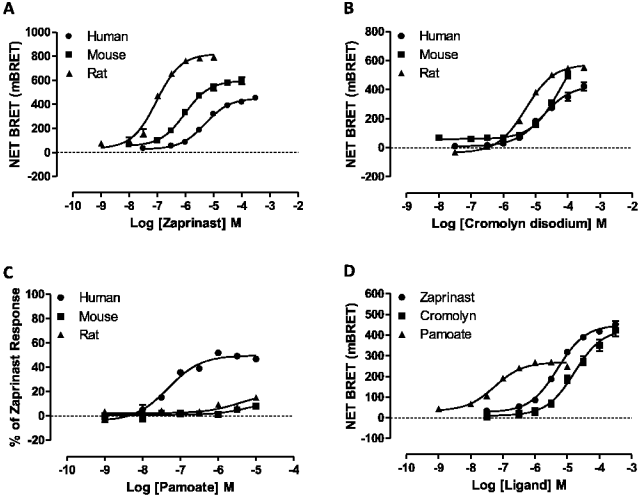
A
NET BRET (mBRET)
Human
Mouse
Rat
Log [Zaprinast] M
B
NET BRET (mBRET)
Human
Mouse
Rat
Log [Cromolyn disodium] M
C
% of Zaprinast Response
Human
Mouse
Rat
Log [Pamoate] M
D
NET BRET (mBRET)
Zaprinast
Cromolyn
Pamoate
Log [Ligand] M

Figure 3

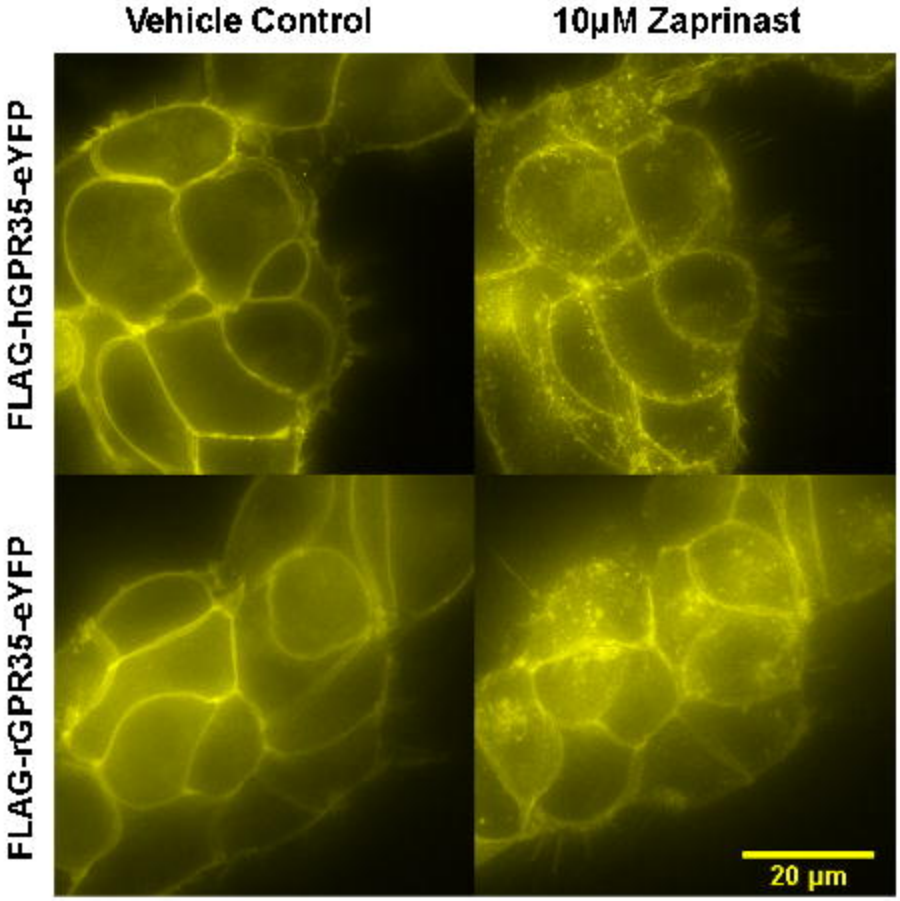
Vehicle Control
10μM Zaprinast
FLAG-hGPR35-eYFP
FLAG-rGPR35-eYFP
20 μm

Figure 4

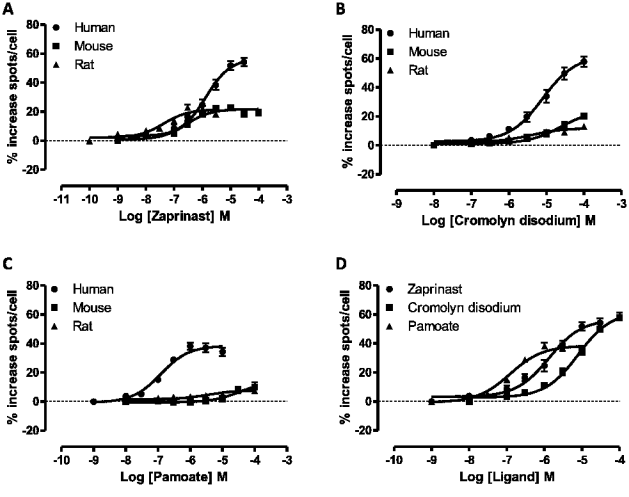
A
Human
Mouse
Rat
% increase spots/cell
Log [Zaprinast] M
B
Human
Mouse
Rat
% increase spots/cell
Log [Cromolyn disodium] M
C
Human
Mouse
Rat
% increase spots/cell
Log [Pamoate] M
D
Zaprinast
Cromolyn disodium
Pamoate
% increase spots/cell
Log [Ligand] M

Figure 5

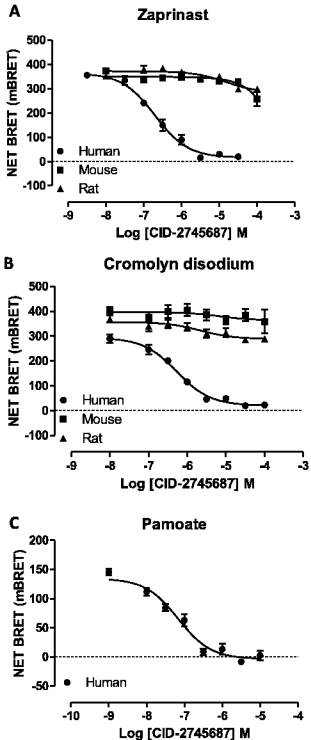
A
Zaprinast
NET BRET (mBRET)
500
400
300
200
100
0
-100
Human
Mouse
Rat
-9
-8
-7
-6
-5
-4
-3
Log [CID-2745687] M
B
Cromolyn disodium
NET BRET (mBRET)
500
400
300
200
100
0
-100
Human
Mouse
Rat
-9
-8
-7
-6
-5
-4
-3
Log [CID-2745687] M
C
Pamoate
NET BRET (mBRET)
200
150
100
50
0
-50
Human
-10
-9
-8
-7
-6
-5
-4
Log [CID-2745687] M

Figure 6

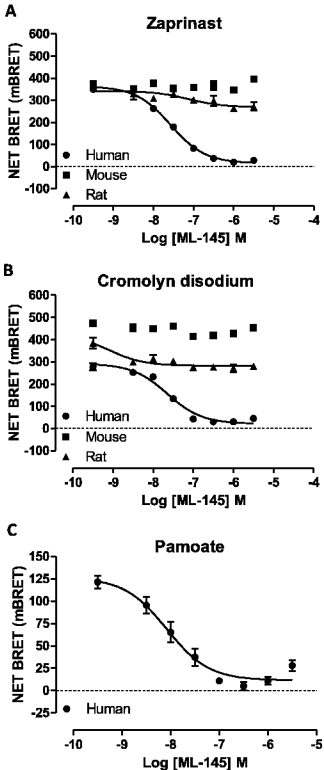
A
Zaprinast
NET BRET (mBRET)
600
500
400
300
200
100
0
-100
Human
Mouse
Rat
-10
-9
-8
-7
-6
-5
-4
Log [ML-145] M
B
Cromolyn disodium
NET BRET (mBRET)
600
500
400
300
200
100
0
-100
Human
Mouse
Rat
-10
-9
-8
-7
-6
-5
-4
Log [ML-145] M
C
Pamoate
NET BRET (mBRET)
150
125
100
75
50
25
0
-25
Human
-10
-9
-8
-7
-6
-5
Log [ML-145] M

Figure 7

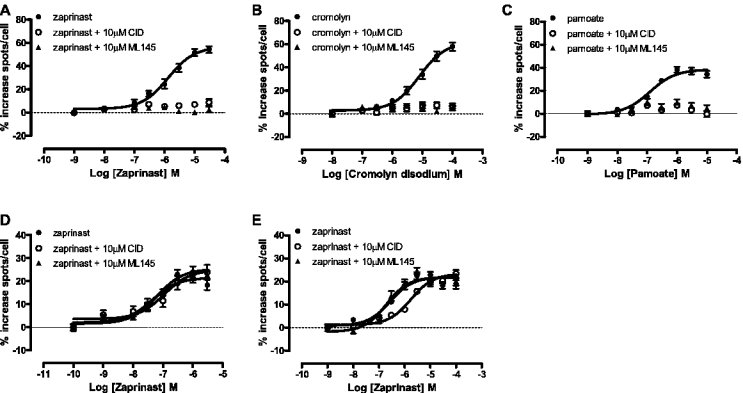
A
zaprinast
zaprinast + 10μM CID
zaprinast + 10μM ML145
% increase spots/cell
Log [Zaprinast] M
B
cromolyn
cromolyn + 10μM CID
cromolyn + 10μM ML145
% increase spots/cell
Log [Cromolyn disodium] M
C
pamoate
pamoate + 10μM CID
pamoate + 10μM ML145
% increase spots/cell
Log [Pamoate] M
D
zaprinast
zaprinast + 10μM CID
zaprinast + 10μM ML145
% increase spots/cell
Log [Zaprinast] M
E
zaprinast
zaprinast + 10μM CID
zaprinast + 10μM ML145
% increase spots/cell
Log [Zaprinast] M

Figure 8

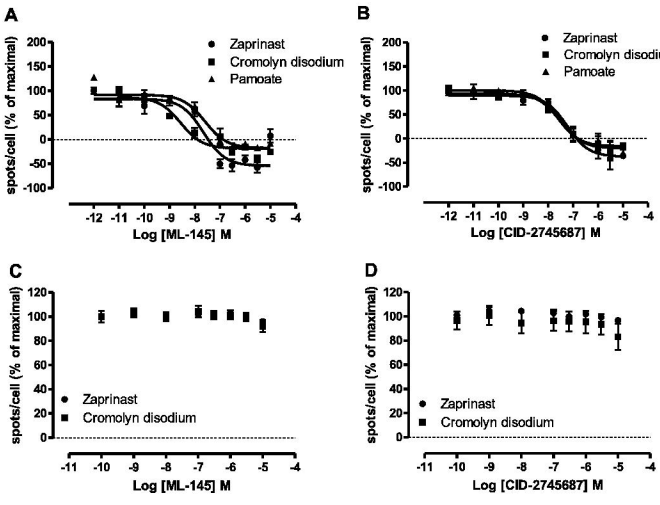
A
B
C
D
spots/cell (% of maximal)
Zaprinast
Cromolyn disodium
Pamoate
Log [ML-145] M
Log [CID-2745687] M

Figure 9

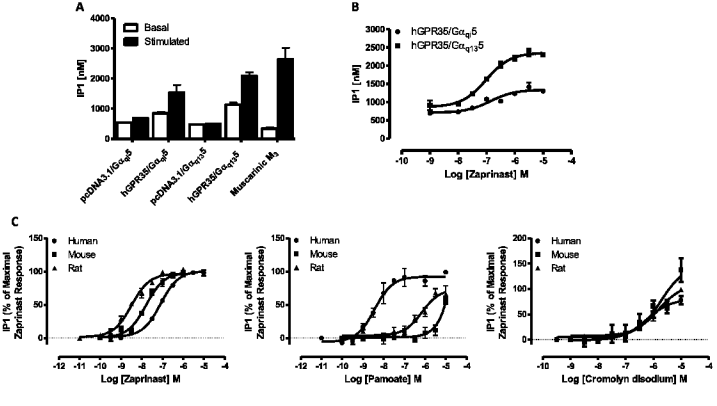
A
Basal
Stimulated
IP1 [nM]
4000
3000
2000
1000
0
pcDNA3.1/Gα$_{qi}$5
hGPR35/Gα$_{qi}$5
pcDNA3.1/Gα$_{q13}$5
hGPR35/Gα$_{q13}$5
Muscarinic M$_3$
B
hGPR35/Gα$_{qi}$5
hGPR35/Gα$_{q13}$5
IP1 [nM]
3000
2500
2000
1500
1000
500
0
-10 -9 -8 -7 -6 -5 -4
Log [Zaprinast] M
C
Human
Mouse
Rat
IP1 (% of Maximal Zaprinast Response)
150
100
50
0
-12 -11 -10 -9 -8 -7 -6 -5 -4
Log [Zaprinast] M
Log [Pamoate] M
Log [Cromolyn disodium] M
200

Figure 10

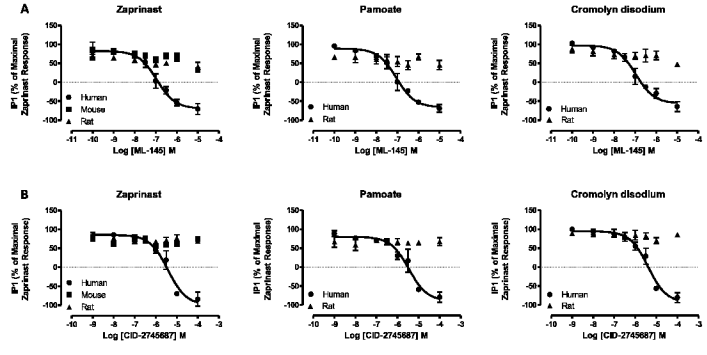
A
Zaprinast
Pamoate
Cromolyn disodium
IP1 (% of Maximal Zaprinast Response)
Human
Mouse
Rat
Log [ML-145] M
B
Log [CID-2745687] M

Figure 11

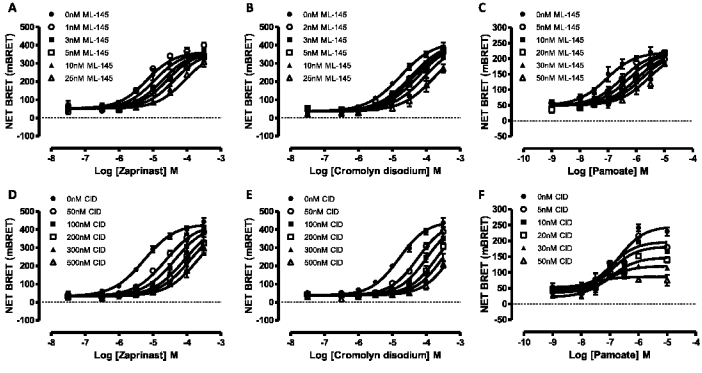
A
0nM ML-145
1nM ML-145
3nM ML-145
5nM ML-145
10nM ML-145
20nM ML-145
NET BRET (mBRET)
Log [Zaprinast] M
B
0nM ML-145
2nM ML-145
3nM ML-145
5nM ML-145
10nM ML-145
20nM ML-145
NET BRET (mBRET)
Log [Cromolyn disodium] M
C
0nM ML-145
5nM ML-145
10nM ML-145
20nM ML-145
30nM ML-145
50nM ML-145
NET BRET (mBRET)
Log [Pamoate] M
D
0nM CID
50nM CID
100nM CID
200nM CID
300nM CID
500nM CID
NET BRET (mBRET)
Log [Zaprinast] M
E
0nM CID
50nM CID
100nM CID
200nM CID
300nM CID
500nM CID
NET BRET (mBRET)
Log [Cromolyn disodium] M
F
0nM CID
5nM CID
10nM CID
20nM CID
30nM CID
50nM CID
NET BRET (mBRET)
Log [Pamoate] M

Figure 12

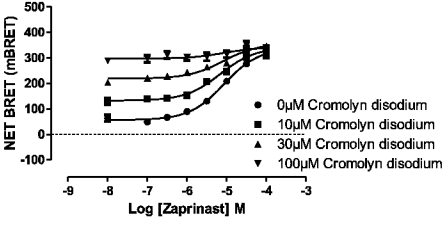
NET BRET (mBRET)
500
400
300
200
100
0
-100
-9
-8
-7
-6
-5
-4
-3
Log [Zaprinast] M
0μM Cromolyn disodium
10μM Cromolyn disodium
30μM Cromolyn disodium
100μM Cromolyn disodium

Figure 13

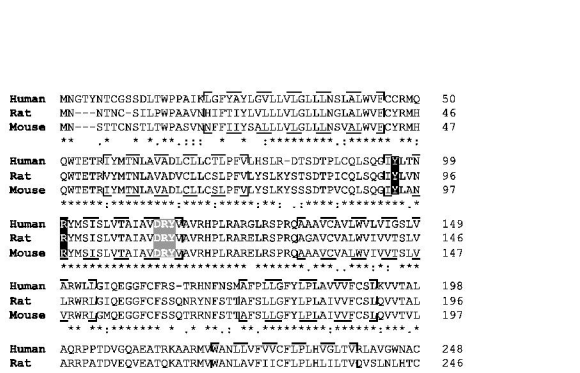
Human MNGTYNTCGSSDLTWPPAIKLGPYAYLGVLLVLGLLLNSLALWVFCCRMQ 50
Rat MN---NTNC-SILPWPAAVNHIFTIYLVLLLVLGLLLNGLALWVFCYRMH 46
Mouse MN---STTCNSTLTWPASVNNFFLIYSALLLVLGLLLNSVALWVFCYRMH 47
Human QWTETRLYMTNLAVADLCLLCTLPFVLHSLR-DTSDTPLCQLSQGIYLTN 99
Rat QWTETRMYMTNLAVADVCLLCSLPFVLYSLKYSTSDTPICQLSQGIYLVN 96
Mouse QWTETRLYMTNLAVADLCLLCSLPFVLYSLKYSSSDTPVCQLSQGIYLAN 97
Human FYMSISLVTAIAVDRYVAVRHPLRARGLRSPRQAAAVCVALWVLVIGSLV 149
Rat FYMSISLVTAIAVDRYVAVRHPLRARELRSPRQAGAVCVALWVIVVTSLV 146
Mouse FYMSISLVTAIAVDRYVAVRHPLRARELRSPRQAAAVCVALWVIVVTSLV 147
Human ARWLLGIQEGGFCFRS-TRHNFNSMAFPLLGFYLPLAVVVFCSLKVVTAL 198
Rat LRWRLGIQEGGFCFSSQNRYNFSTIAFSLLGFYLPLAIVVFCSLQVVTAL 196
Mouse VRWRLGMQEGGFCFSSQTRRNFSTIAFSLLGFYLPLAIVVFCSLQVVTVL 197
Human AQRPPTDVGQAEATRKAARMVWANLLVFVVCFLPLHVGLTVRLAVGWNAC 248
Rat ARRPATDVEQVEATQKATRMVWANLAVFIICFLPLHLILTVQVSLNLHTC 246
Mouse SRRPAADVGQAEATQKATHMVWANLAVFVICFLPLHVVLTVQVSLNLNTC 247
Human ALLETIRRALYIFSKLSDANCCLDAICYYYMAKEFQEASALAVAPRAKAH 298
Rat AARNIFSRALTIFTAKLSDINCCLDAICYYYMAKEFQDASLRATAS-STPH 295
Mouse AARDTFSRALSIFGKLSDTNCCLDAICYYYMAREFQEASKPATSS-NTPH 296
Human KSQDSLCVTLA 309
Rat KSQDTQSLSLT 306
Mouse KSQDSQILSLT 307